Orientation Dependence of the Photochemical Reactivity of $BaTi_4O_9$

Jennifer L. Giocondi, Shahrzad Samadzadeh, and Gregory S. Rohrer
Department of Materials Science and Engineering, Carnegie Mellon University,
Pittsburgh, PA 15213-3890, U.S.A.

ABSTRACT

$BaTi_4O_9$ is a photocatalyst with a pentagonal prism tunnel structure. It has been hypothesized that the tunnels promote the separation of photogenerated carriers and, therefore, lead to the spatial separation of oxidation and reduction half reactions. This hypothesis has been tested by observing the distribution of reduced and oxidized reaction products on $BaTi_4O_9$ surfaces over a wide range of orientations. The surface orientations were determined by electron backscattered diffraction and atomic force microscopy was used to examine the structure of the surface both before and after the deposition of reaction products. Reduction products (Ag^0) are distributed uniformly. The distribution of oxidation products (PbO_2) is also not correlated to the surface orientation or to the orientation of the tunnels with respect to the surface. Based on these observations, we conclude that the tunnels in this structure do not separate photogenerated charge carriers and that this mechanism is not responsible for this compound's relatively high photocatalytic activity.

INTRODUCTION

Heterogeneous photochemical reactions can occur on ceramic surfaces when the adsorption of light with an energy greater than the band gap creates electrons and holes that migrate to the solid surface where they can participate in reactions with adsorbed species. One goal of photochemistry research during the past three decades has been to promote the efficient photolysis of water using particulate oxide catalysts [1]. The efficient photoassisted decomposition of water into hydrogen and oxygen gas is a promising means of converting solar energy into clean burning fuel (H_2 gas). The recombination of photogenerated carriers and the back reaction of H_2 and O_2 to reform water are frequently cited as factors limiting the efficiency of photolysis using particulate materials. For this reason, recent work has been directed toward the development of catalyst structures that separate the charge carriers and the H_2 and O_2 production sites [2].

Oxides with highly anisotropic crystal structures have attracted attention in the search for efficient water photolysis catalysts. The best (most efficient) materials have been found to have layered [3,4] or tunnel [5-9] structures and previous workers speculated that this was the key to their high efficiencies [2, 4, 9]. They hypothesize that the reduction and oxidation functions of the catalyst occur at different elements of the structure and, by producing the reduced and oxidized products at separate locations, the rate of the back reaction is suppressed and the overall H_2 production efficiency increased. Our objective was to test this hypothesis by measuring the orientation dependence of reduction and oxidation reactions on $BaTi_4O_9$, a material with a pentagonal prism tunnel structure (Pmmn, a = 14.53 Å, b = 3.79 Å, c = 6.29 Å) [10]. If the reactivity depends on the inclination of the surface plane with respect to the tunnels, then the hypothesis is supported. If not, then the surface sites associated with the tunnels are not likely to be solely responsible for the catalyst's high efficiency.

The experimental approach is based on the use of photochemical probe reactions that leave insoluble products on the surface at the sites of oxidation and reduction [11,12]. The locations of the reaction sites are determined by examining the surfaces before and after the photochemical probe reaction using atomic force microscopy (AFM) [13]. Polycrystals are used to examine the activity over the range of all crystallographic orientations and electron backscattered diffraction patterns (EBSPs) are used to determine the orientations of individual grains. The amount of reaction product observed on each grain is taken as a measure its reactivity and by correlating these observations to the surface orientation, the anisotropy of the reactivity is determined [14].

EXPERIMENTAL DETAILS

$BaTi_4O_9$ was synthesized by reacting stoichiometric amounts of $BaCO_3$ and TiO_2 powders at 1250 °C for 20 h. After confirming phase purity by X-ray diffraction, the $BaTi_4O_9$ power was uniaxially compacted under 150 MPa to form disk-shaped pellets with a thickness of 12 mm and an approximate diameter of 11 mm. The pellets were then placed in an alumina crucible with an excess of the parent powder to insure that the pellet did not contact the crucible. The samples were then heated to 875 °C (all ramp rates were 10 °C / min) for 10 h in air to burn off any residual organics, sintered for 10 h at 1150 °C, and the grains were grown for 53 h at 1330 °C.

The sintered samples were then lapped flat using a 3 μm Al_2O_3 (Buehler) aqueous solution and polished with a basic 0.02 μm colloidal silica solution (Buehler). Polished samples were annealed in air at 900 °C for 6 h to remove polishing damage, facet the surface, and thermally etch the grain boundaries. The average grain size was 20 μm.

The photochemical reactions on the $BaTi_4O_9$ samples was carried out in the following way. A viton O-ring, 1.7 mm thick, was placed on the sample surface and the interior volume was filled with a silver (0.115 M aqueous $AgNO_3$ (Fisher Scientific)) or lead (0.0115 M aqueous $Pb(C_2H_3O_2)_2$ (Fisher Scientific)) bearing solution. A 0.2 mm thick quartz cover slip was then placed on top of the O-ring and held in place by the surface tension of the solution. The sample was illuminated using a 400 W Hg lamp for 3 sec (silver reduction) or 150 sec (lead oxidation) and then rinsed with deionized H_2O and dried with forced air. In control experiments conducted with light made up of energies less than barium tetratitanate's band gap, no photochemical reactions were observed. Other control experiments using silica or alumina in place of $BaTi_4O_9$ did not yield a PbO_2 product.

Atomic Force Microscopy (AFM) (Thermomicroscopes M5) was used to examine the surface topography both before and after the probe reactions. In this way, reaction sites, indicated by the presence of solid products, could be directly correlated to preexisting surface features. Gold-coated, sharpened pyramidal Si_3N_4 probes (Thermomicroscopes ML06E) were used for images obtained before the reaction in contact mode. The force used varied between 1-2 nN. Non-contact AFM (NC-AFM) was used to examine the surfaces following the silver reaction. Conical Si probes (Thermomicroscopes UL20A/B) with resonant frequencies between 70 – 100 kHz were used for the NC-AFM images. All topographs presented in this document are displayed in grayscale; light contrast indicates relatively high regions of the surface while dark contrast indicates relatively low areas of the surface.

After the AFM imaging was completed, the crystallographic orientations of individual grains in the polycrystalline samples were determined from electron backscattered diffraction patterns (EBSP). The samples were imaged in a Phillips XL40FEG scanning electron microscope. An EBSP was collected for each grain and the patterns were indexed using

Orientation Imaging Microscopy Software, version 3 (TexSEM Laboratories, Inc.). The software returns a set of Euler angles (ϕ_1, Φ, ϕ_2) for each grain which are used to specify a relationship between the sample reference frame and the crystallographic axes. From these data, the components of the surface normals can be computed. Because some crystal orientations facet during the anneal at 900°C, the surface normals computed from the EBSPs do not necessarily correlate to the crystallographic planes that bound the surface.

RESULTS

The topographic AFM image in Fig. 1a shows the surface of the $BaTi_4O_9$ polycrystal before any reaction. In general, the surfaces are smooth so that the macroscopic surface orientation represents the actual surface orientation. In some cases (for example, the grain labeled 7), the surfaces are faceted and the actual facets bounding the surface are not the same as the macroscopic surface orientation. Of the more than 50 grains examined, approximately 25 % are faceted. The distribution of faceted orientations is illustrated in Fig. 2a.

When exposed to light in the presence of $AgNO_3$, the surfaces of all of the grains were coated by silver, with no detectable orientation dependence. On the other hand, the reduced rate of the lead oxidation process allowed spatial variations to be detected. The topographic AFM image in Fig. 1b shows the same area as Fig. 1a after the photochemical oxidation of lead. The oxidized lead deposits appear as the white contrast in the AFM image. Some variation in the rate of lead oxidation is obvious. For example, grains labeled 4 and 6 have more deposits than the grains labeled 2 and 5. Similar observations were made on more than 50 grains, and the
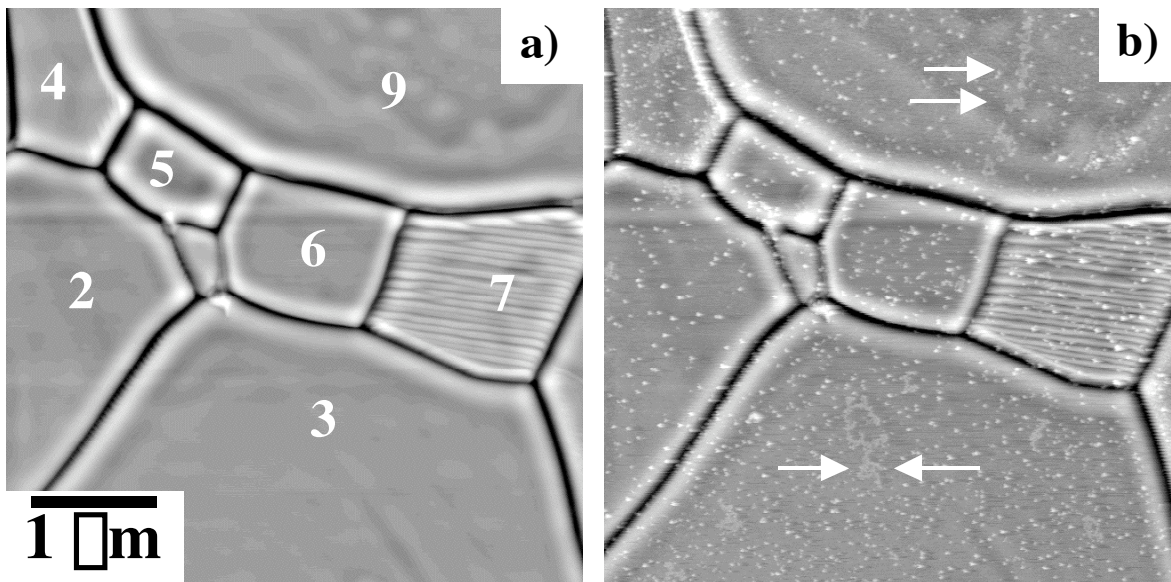

Figure 1. Topographic AFM images of the surfaces of crystallites in a $BaTi_4O_9$ polycrystal before and after illumination in a lead acetate solution. (a) Contact AFM image of eight grains (2 – 9) before the reaction. (b) NC-AFM image of the same area following the reaction. The areas of white contrast correspond to PbO_2 deposits. Continuous networks of reaction products are indicated by the arrows. The vertical black-to-white contrast in (a) and (b) are 15 nm and 20 nm, respectively.
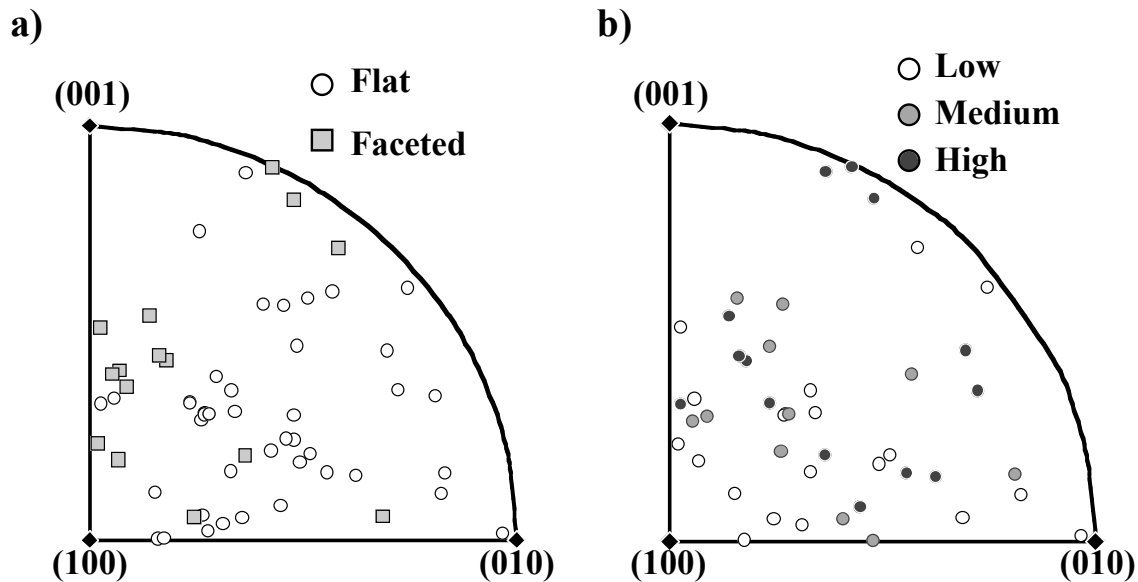
a)

b)

Figure 2. (a) An inverse pole figure plotted on the standard stereographic triangle for orthorhombic crystals, showing the orientations of smooth and faceted grains. The black diamonds indicate the locations of low index orientations. (b) Inverse pole figure illustrating the relative reactivity of each grain as a function of orientation.

reactivities are classified as high (> 18 deposits /μm^2), medium (10 - 18 deposits /μm^2), or low (< 10 deposits /μm^2). These results are summarized in Fig. 2b.

There are several noteworthy features of these results. First, the differences in the amount of reaction products found on different grains is not as large as observed in previous studies of TiO_2 [14]. In the earlier studies, some grains were completely covered with reaction products while others were nearly free of products. By comparison, this reaction exhibits little anisotropy. Second, the differences in the reactivity within a single grain are almost as large as the differences between grains. For example, the arrows in Fig. 1b point to continuous networks of lead oxide deposits while the remainder of the deposits on the same grain are isolated. Finally, when the orientation dependence of the reactivity is examined, there are no distinct trends. Similar orientations can have very different reactivities and there are no clear trends in the plot of reactivity versus orientation. Finally, the data in Fig. 2 also indicate that the rate of reaction is not correlated to either the presence of smooth surfaces or facets on the grains.

DISCUSSION

The experiments described here were carried out to determine if the reactivity of $BaTi_4O_9$ was correlated to the orientations of the tunnels in the structure. The structure is illustrated in Fig. 3, which shows that the tunnels are oriented along the [010] axis of the crystal. This means that crystals exposing (010) planes reveal the maximum number of tunnel openings while those crystals with orientations along the line connecting (100) and (001) are parallel to the tunnel direction (see Fig. 2). The reactivity does not seem to be correlated with these special orientations. This can be seen most clearly in Fig. 4. The surface of grain 5 is nearly perpendicular to the [010] direction so that this crystal exposes the highest density of tunnel sites. On the other hand, grains 7 and 2 expose surfaces that are nearly parallel to the tunnels. The
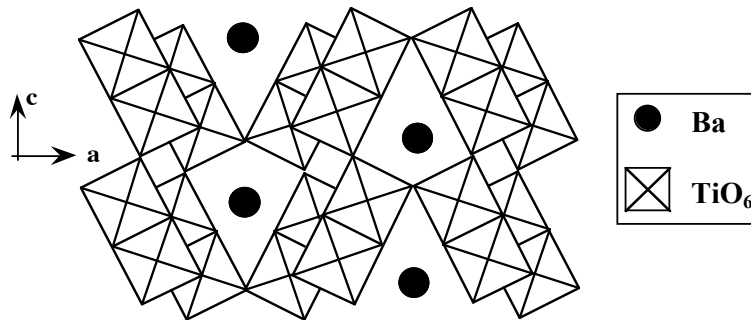
Figure 3. Schematic drawing of the pentagonal prism tunnel structure (Pmmn) parallel to [010]. The black circles represent Ba atoms that are surrounded by TiO_6 octahedra.
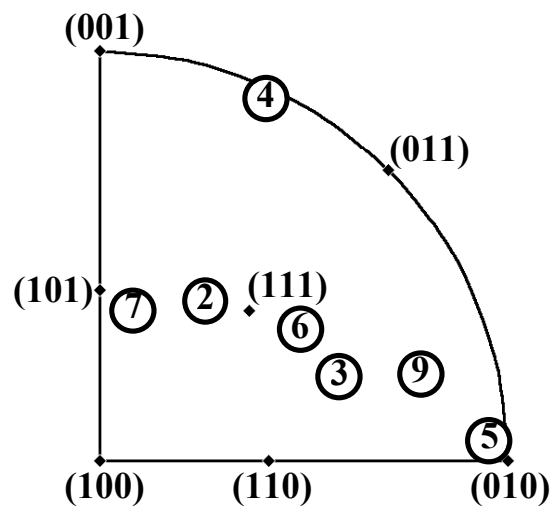

Figure 4. Inverse pole figure illustrating the orientations of the grains in Figure 1. Note that the surface of grain 5 is nearly perpendicular to the tunnels.

AFM image in Fig. 1b indicates that reactivities of grains 5, 7, and 2 are not significantly different.

The results from both the reduction and oxidation experiments refute the hypothesis that sites associated with the tunnels in some way spatially isolate either the reduction or oxidation half reactions. The original proposal was that distortions in the octahedral units surrounding the pentagonal tunnels create large dipole moments that are directed towards the center of the tunnels and it is these internal electric fields that separate the photogenerated charges [9, 15]. The proposal for charge separation by dipolar fields is not unreasonable. Previous studies of the ferroelectric $(Pb,K)_2Nb_2O_6$ indicated that poling influences its photochemical activity [16] and recent studies of $BaTiO_3$ show that polarizations in ferroelectric domains influence the transport of photogenerated carriers and lead to the spatial separation of reaction products [13, 17]. It has also recently been observed that dipolar fields associated with polar surface terminations of the non-ferroelectric $SrTiO_3$ influence the transport of carriers to the surface and this also leads to a spatial separation of the photochemical oxidation and reduction reactions [18]. Since localized variations in the reactivity on single grains observed in the current study are similar to variations observed on $SrTiO_3$ surfaces, it is possible that localized changes in the surface termination are responsible for the inhomogeneous distribution of oxidized products on $BaTi_4O_9$ surfaces.

CONCLUSIONS

Observations of the spatial distribution of reduction and oxidation products on $BaTi_4O_9$ surfaces lend no support to the hypothesis that dipolar fields associated with the tunnels in this structure lead to a separation of charge carriers and the spatial isolation of one of the half reactions. Surfaces perpendicular and parallel to the tunnels have similar reactivities.

ACKNOWLEDGEMENTS

REFERENCES

[1] A. Fujishima and K. Honda, Nature **238**, 37 (1972).
[2] K. Domen, in *Surface Photochemistry*, edited by M. Anpo, (J. Wiley and Sons, Chichester, England, 1996) p. 1.
[3] T. Takata, Y. Furumi, K. Shinohara, A. Tanaka, M. Hara, J.N. Kondo, and K. Domen, Chem. Mat. **9**, 1063 (1997).
[4] D.W.Hwang, H.G. Kim, J. Kim, K.Y. Cha, Y.G. Kim, and J.S. Lee, J. Catalysis **193**, 40 (2000).
[5] Y. Inoue, T. Kubokawa, and K. Sato, J. Phys. Chem. **95**, 4059 (1991).
[6] S. Ogura, M. Kohno, K. Sato, and Y. Inoue, Phys. Chem. Chem. Phys. **1**, 179 (1999).
[7] Y. Inoue, T. Niiyama, Y. Asai, and K. Sato, J. Chem. Soc., Chem. Commun. *1992*, 579.
[8] M. Kohno, S. Ogura, K. Sato, and Y. Inoue, J. Chem. Soc., Faraday Trans. **93** (14), 2433 (1997).
[9] M. Kohno, S. Ogura, K. Sato, and Y. Inoue, in *Studies in Surface Science and Catalysis*, Vol. 101, edited by J.W. Hightower, W.N. Delgass, E. Iglesia, and A.T. Bell, (Elsevier Science, New York, 1996) p. 143.
[10] E. Tillmanns and W.H. Baur, Acta Crystallogr., Sect. B **26**, 1645 (1970).
[11] J. Torres and S. Cervera-March, Chem. Eng. Sci. **47**, 3857 (1992).
[12] J.-M. Herrmann, J. Disdier, and P. Pichat, J. Catalysis **113** (1), 72 (1988).
[13] J.L. Giocondi and G.S. Rohrer, J. Phys. Chem. B **105** (35), 8275 (2001).
[14] J.B. Lowekamp, G.S. Rohrer, P.A. Morris Hotsenpiller, J.D. Bolt, and W.D. Farneth, J. Phys. Chem. B **102** (38), 7323 (1998).
[15] M. Kohno, S. Ogura, K. Sato, and Y. Inoue, J. Chem. Soc., Faraday Trans. **94** (1), 89 (1998).
[16] Y. Inoue, O. Hayashi, and K. Sato, J. Chem. Soc., Faraday Trans. **86** (12), 2277 (1990).
[17] J.L. Giocondi and G.S. Rohrer, Chem. Mater. **13** (2), 241 (2001).
[18] J.L. Giocondi and G.S. Rohrer, J. Amer. Ceram. Soc., submitted.